

A novel four variable refined plate theory for bending, buckling, and vibration of functionally graded plates

Habib Hebali^{1,2}, Ahmed Bakora², Abdelouahed Tounsi^{*2,3} and Abdelhakim Kaci^{2,4}

¹ Université Ibn Khaldoun, BP 78 Zaaroura, 14000 Tiaret, Algérie

² Material and Hydrology Laboratory, University of Sidi Bel Abbès, Faculty of Technology, Civil Engineering Department, Algeria

³ Laboratoire de Modélisation et Simulation Multi-échelle, Département de Physique, Faculté des Sciences Exactes, Département de Physique, Université de Sidi Bel Abbès, Algeria

⁴ Department of Civil Engineering and Hydraulics, University Dr. Taher Moulay of Saida, Algeria

(Received May 30, 2016, Revised September 22, 2016, Accepted October 02, 2016)

Abstract. This work presents a bending, buckling, and vibration analysis of functionally graded plates by employing a novel higher-order shear deformation theory (HSDT). This theory has only four unknowns, which is even less than the first shear deformation theory (FSDT). A shear correction coefficient is, thus, not needed. Unlike the conventional HSDT, the present one has a new displacement field which introduces undetermined integral variables. Equations of motion are obtained by utilizing the Hamilton's principles and solved via Navier's procedure. The convergence and the validation of the proposed theoretical numerical model are performed to demonstrate the efficacy of the model.

Keywords: bending; buckling; vibration; functionally graded plate; plate theory

1. Introduction

In 1984, the concept of functionally graded materials (FGMs) was first proposed. FGM is a class of composite material in which material characteristics continuously change between two surfaces, thus eliminating the stress concentration phenomenon, which is a characteristic phenomenon found in laminated composite materials. FGMs are widely used in many engineering applications such as spacecraft industry, mechanics, civil engineering, aerospace, nuclear, automotive and so on (Lu *et al.* 2009, Liang *et al.* 2014, 2015, Bouguenina *et al.* 2015, Pradhan and Chakraverty 2015, Sofiyev and Kuruoglu 2015, Kar and Panda 2015, Kirkland and Uy 2015, Ebrahimi and Dashti 2015, Ebrahimi and Habibi 2016, Cunedioğlu 2015, Meradjah *et al.* 2015, Bouguenina *et al.* 2015, Darılmaz 2015, Bellifa *et al.* 2016). Presenting new characteristics, FGMs have also attracted intensive research interests, which were mainly focused on their bending, buckling and vibration characteristics of functionally graded (FG) structures (Neves *et al.* 2013, Eltahir *et al.* 2013a, b, 2014a, b, Swaminathan and Naveenkumar 2014, Bousahla *et al.* 2014, Akbaş 2015, Tung 2015, Ait Yahia *et al.* 2015, Bourada *et al.* 2015, Ait Amar Meziane *et al.* 2014,

*Corresponding author, Professor, E-mail: tou_abdel@yahoo.com

Al-Basyouni *et al.* 2015, Arefi 2015, Belabed *et al.* 2014, Larbi Chaht *et al.* 2015). Indeed, many computational theories have been proposed for investigating the behavior of FG structures. In general, these mathematical models can be defined into three main categories: classical plate theory (CPT); first-order shear deformation theory (FSDT); and higher-order shear deformation theory (HSDT).

The CPT, which ignores the transverse shear deformation influences, produces reasonable results for thin plates. The CPT has been employed for the bending, buckling, and vibration investigations of plates via analytical formulation (Leissa 1973, Leissa and Kang 2002, Kang and Leissa 2005) and numerical formulation (Eisenberger and Alexandrov 2003, Wang *et al.* 2006, Liu and Li 2010). For moderately thick plates, the CPT under-predicts deflections and over-predicts buckling loads as well as natural frequencies. The FSDT considers the transverse shear deformation influence, but introduces a shear correction parameter to respect the free transverse shear stress conditions on the external surfaces of the plate (Della Croce and Venini 2004, Ganapathi *et al.* 2006, Zhao and Liew 2009, Zhao *et al.* 2009, Lee *et al.* 2010, Hosseini-Hashemi *et al.* 2010, 2011a). Although the FSDT predicts a reasonable description of behavior for thin to moderately thick plates, it is not practical to employ due to difficulty in assessing of correct value of the shear correction parameter. To overcome the employ of shear correction parameter, many HSDTs were proposed with the pretention of nonlinear distributions of in-plane displacements within the plate thickness, notable among them are Reddy (2000), Karama *et al.* (2003), Xiao *et al.* (2007), Matsunaga (2008), Pradyumna and Bandyopadhyay (2008), Fares *et al.* (2009), Talha and Singh (2010, 2011), Boudierba *et al.* (2013), Hebali *et al.* (2014), Mahi *et al.* (2015), Bennai *et al.* (2015), Xiang *et al.* (2011), Tounsi *et al.* (2013), Zidi *et al.* (2014), Bounouara *et al.* (2016), Bousahla *et al.* (2016), Boukhari *et al.* (2016) and Boudierba *et al.* (2016). Carrera *et al.* (2010) presented refined and advanced models for multilayered plates and shells embedding functionally graded material layers. Cinefra and Soave (2011) proposed an accurate vibration analysis of multilayered plates made of functionally graded materials. Ait Atmane *et al.* (2015) presented a computational shear displacement model for vibrational analysis of FG beams with porosities. Akavci (2015) presented an efficient shear deformation theory for free vibration of FG thick rectangular plates on elastic foundation. Using various four variable refined plate theories, Attia *et al.* (2015) studied the free vibration analysis of FG plates with temperature-dependent properties. Bakora and Tounsi (2015) investigated the thermo-mechanical post-buckling behavior of thick FG plates resting on elastic foundations. Beldjelili *et al.* (2016) analyzed the hygro-thermo-mechanical bending response of S-FGM plates resting on variable elastic foundations using a four-variable trigonometric plate theory. Belkorissat *et al.* (2015) discussed the vibration properties of FG nanoplate using a new nonlocal refined four variable model. Hamidi *et al.* (2015) developed a sinusoidal plate theory with 5-unknowns and stretching effect for thermomechanical bending of FG sandwich plates. Bennoun *et al.* (2016) presented a novel five variable refined plate theory for dynamic analysis of FG sandwich plates. Recently, Tounsi *et al.* (2016) proposed a new 3-unknowns non-polynomial plate theory for buckling and vibration of FG sandwich plate. In the same way, Houari *et al.* (2016) proposed also a novel simple three -unknown sinusoidal shear deformation theory for FG plates.

In the present work, a new displacement field is proposed by considering higher-order variations of in-plane displacements through the plate thickness and the novel constructed displacement field is applied to investigate the bending, buckling, and vibration response of FG plates. The incorporation of the integral term in the plate kinematics led to a reduction in the number of variables and equations of motion. Numerical results are considered to check the

accuracy of the developed theory in predicting the bending, buckling, and vibration behaviors of FG plates.

2. Theory and formulation

The FG plate is composed by a mixture of ceramic and metal components whose material characteristics change across the plate thickness with a power law distribution of the volume fractions of the constituents of the two materials as

$$P(z) = P_m + (P_c - P_m) \left(\frac{1}{2} + \frac{z}{h} \right)^p \tag{1}$$

where P denotes the effective material characteristic such as Young’s modulus E and mass density ρ subscripts m and c denote the metallic and ceramic components, respectively; and p is the power law exponent. The value of p equal to zero indicates a fully ceramic plate, whereas infinite p represents a fully metallic plate. Since the influences of the variation of Poisson’s ratio ν on the behavior of FG plates are very small (Yang *et al.* 2005, Kitipornchai *et al.* 2006), it is supposed to be constant for convenience.

2.1 Kinematics and strains

In this article, further simplifying supposition are made to the conventional HSDT so that the number of unknowns is reduced. The displacement field of the conventional HSDT is given by (Bouchafa *et al.* 2015)

$$u(x, y, z, t) = u_0(x, y, t) - z \frac{\partial w_0}{\partial x} + f(z) \varphi_x(x, y, t) \tag{2a}$$

$$v(x, y, z, t) = v_0(x, y, t) - z \frac{\partial w_0}{\partial y} + f(z) \varphi_y(x, y, t) \tag{2b}$$

$$w(x, y, z, t) = w_0(x, y, t) \tag{2c}$$

where u_0 ; v_0 ; w_0 , φ_x , φ_y are five unknown displacements of the mid-plane of the plate, $f(z)$ denotes shape function representing the variation of the transverse shear strains and stresses within the thickness. By considering that $\varphi_x = \int \theta(x, y) dx$ and $\varphi_y = \int \theta(x, y) dy$, the displacement field of the present model can be expressed in a simpler form as (Bourada *et al.* 2016)

$$u(x, y, z, t) = u_0(x, y, t) - z \frac{\partial w_0}{\partial x} + k_1 f(z) \int \theta(x, y, t) dx \tag{3a}$$

$$v(x, y, z, t) = v_0(x, y, t) - z \frac{\partial w_0}{\partial y} + k_2 f(z) \int \theta(x, y, t) dy \tag{3b}$$

$$w(x, y, z, t) = w_0(x, y, t) \tag{3c}$$

In this work, the present higher-order shear deformation plate theory is obtained by setting

$$f(z) = z \left(\frac{5}{4} - \frac{5z^2}{3h^2} \right) \quad (4)$$

It can be seen that the displacement field in Eq. (3) introduces only four unknowns (u_0 , v_0 , w_0 and θ). The nonzero strains associated with the displacement field in Eq. (3) are

$$\begin{Bmatrix} \varepsilon_x \\ \varepsilon_y \\ \gamma_{xy} \end{Bmatrix} = \begin{Bmatrix} \varepsilon_x^0 \\ \varepsilon_y^0 \\ \gamma_{xy}^0 \end{Bmatrix} + z \begin{Bmatrix} k_x^b \\ k_y^b \\ k_{xy}^b \end{Bmatrix} + f(z) \begin{Bmatrix} k_x^s \\ k_y^s \\ k_{xy}^s \end{Bmatrix}, \quad \begin{Bmatrix} \gamma_{yz} \\ \gamma_{xz} \end{Bmatrix} = g(z) \begin{Bmatrix} \gamma_{yz}^0 \\ \gamma_{xz}^0 \end{Bmatrix}, \quad (5)$$

where

$$\begin{Bmatrix} \varepsilon_x^0 \\ \varepsilon_y^0 \\ \gamma_{xy}^0 \end{Bmatrix} = \begin{Bmatrix} \frac{\partial u_0}{\partial x} \\ \frac{\partial v_0}{\partial x} \\ \frac{\partial u_0}{\partial y} + \frac{\partial v_0}{\partial x} \end{Bmatrix}, \quad \begin{Bmatrix} k_x^b \\ k_y^b \\ k_{xy}^b \end{Bmatrix} = \begin{Bmatrix} -\frac{\partial^2 w_0}{\partial x^2} \\ -\frac{\partial^2 w_0}{\partial y^2} \\ -2\frac{\partial^2 w_0}{\partial x \partial y} \end{Bmatrix}, \quad (6a)$$

$$\begin{Bmatrix} k_x^s \\ k_y^s \\ k_{xy}^s \end{Bmatrix} = \begin{Bmatrix} k_1 \theta \\ k_2 \theta \\ k_1 \frac{\partial}{\partial y} \int \theta dx + k_2 \frac{\partial}{\partial x} \int \theta dy \end{Bmatrix}, \quad \begin{Bmatrix} \gamma_{yz}^0 \\ \gamma_{xz}^0 \end{Bmatrix} = \begin{Bmatrix} k_2 \int \theta dy \\ k_1 \int \theta dx \end{Bmatrix},$$

and

$$g(z) = \frac{df(z)}{dz} \quad (6b)$$

The integrals defined in the above equations shall be resolved by a Navier type method and can be written as follows

$$\frac{\partial}{\partial y} \int \theta dx = A' \frac{\partial^2 \theta}{\partial x \partial y}, \quad \frac{\partial}{\partial x} \int \theta dy = B' \frac{\partial^2 \theta}{\partial x \partial y}, \quad \int \theta dx = A' \frac{\partial \theta}{\partial x}, \quad \int \theta dy = B' \frac{\partial \theta}{\partial y}, \quad (7)$$

where the coefficients A' and B' are expressed according to the type of solution used, in this case via Navier. Therefore, A' , B' , k_1 and k_2 are expressed as follows

$$A' = -\frac{1}{\alpha^2}, \quad B' = -\frac{1}{\beta^2}, \quad k_1 = \alpha^2, \quad k_2 = \beta^2 \quad (8)$$

where α and β are defined in expression (24).

For elastic and isotropic FGMs, the constitutive relations can be expressed as

$$\begin{Bmatrix} \sigma_x \\ \sigma_y \\ \tau_{xy} \\ \tau_{yz} \\ \tau_{xz} \end{Bmatrix} = \begin{bmatrix} C_{11} & C_{12} & 0 & 0 & 0 \\ C_{12} & C_{22} & 0 & 0 & 0 \\ 0 & 0 & C_{66} & 0 & 0 \\ 0 & 0 & 0 & C_{44} & 0 \\ 0 & 0 & 0 & 0 & C_{55} \end{bmatrix} \begin{Bmatrix} \varepsilon_x \\ \varepsilon_y \\ \gamma_{xy} \\ \gamma_{yz} \\ \gamma_{xz} \end{Bmatrix} \quad (9)$$

where $(\sigma_x, \sigma_y, \tau_{xy}, \tau_{yz}, \tau_{xz})$ and $(\varepsilon_x, \varepsilon_y, \gamma_{xy}, \gamma_{yz}, \gamma_{xz})$ are the stress and strain components, respectively. Using the material properties defined in Eq. (1), stiffness coefficients, C_{ij} , can be given as

$$C_{11} = C_{22} = \frac{E(z)}{1-\nu^2}, \quad C_{12} = \frac{\nu E(z)}{1-\nu^2}, \quad C_{44} = C_{55} = C_{66} = \frac{E(z)}{2(1+\nu)}, \quad (10)$$

2.2 Equations of motion

Hamilton's principle is herein utilized to determine the equations of motion

$$0 = \int_0^t (\delta U + \delta V - \delta K) dt \quad (11)$$

where δU is the variation of strain energy; δV is the variation of the external work done by external load applied to the plate; and δK is the variation of kinetic energy.

The variation of strain energy of the plate is given by

$$\begin{aligned} \delta U &= \int_V [\sigma_x \delta \varepsilon_x + \sigma_y \delta \varepsilon_y + \tau_{xy} \delta \gamma_{xy} + \tau_{yz} \delta \gamma_{yz} + \tau_{xz} \delta \gamma_{xz}] dV \\ &= \int_A [N_x \delta \varepsilon_x^0 + N_y \delta \varepsilon_y^0 + N_{xy} \delta \gamma_{xy}^0 + M_x^b \delta k_x^b + M_y^b \delta k_y^b + M_{xy}^b \delta k_{xy}^b \\ &\quad + M_x^s \delta k_x^s + M_y^s \delta k_y^s + M_{xy}^s \delta k_{xy}^s + S_{yz}^s \delta \gamma_{yz}^s + S_{xz}^s \delta \gamma_{xz}^0] dA = 0 \end{aligned} \quad (12)$$

where A is the top surface and the stress resultants N , M , and S are defined by

$$(N_i, M_i^b, M_i^s) = \int_{-h/2}^{h/2} (1, z, f) \sigma_i dz, \quad (i = x, y, xy) \quad \text{and} \quad (S_{xz}^s, S_{yz}^s) = \int_{-h/2}^{h/2} g(\tau_{xz}, \tau_{yz}) dz \quad (13)$$

The variation of the external work can be expressed as

$$\delta V = - \int_A q \delta w_0 dA - \int_A \left(N_x^0 \frac{\partial w_0}{\partial x} \frac{\partial \delta w_0}{\partial x} + 2N_{xy}^0 \frac{\partial w_0}{\partial x} \frac{\partial \delta w_0}{\partial y} + N_y^0 \frac{\partial w_0}{\partial y} \frac{\partial \delta w_0}{\partial y} \right) dA \quad (14)$$

where q and (N_x^0, N_y^0, N_{xy}^0) are transverse and in-plane applied loads, respectively.

The variation of kinetic energy of the plate can be expressed as

$$\begin{aligned}
\delta K &= \int_V [\dot{u} \delta \dot{u} + \dot{v} \delta \dot{v} + \dot{w} \delta \dot{w}] \rho(z) dV \\
&= \int_A \left\{ I_0 [\dot{u}_0 \delta \dot{u}_0 + \dot{v}_0 \delta \dot{v}_0 + \dot{w}_0 \delta \dot{w}_0] \right. \\
&\quad - I_1 \left(\dot{u}_0 \frac{\partial \delta \dot{w}_0}{\partial x} + \frac{\partial \dot{w}_0}{\partial x} \delta \dot{u}_0 + \dot{v}_0 \frac{\partial \delta \dot{w}_0}{\partial y} + \frac{\partial \dot{w}_0}{\partial y} \delta \dot{v}_0 \right) \\
&\quad + J_1 \left((k_1 A') \left(\dot{u}_0 \frac{\partial \delta \dot{\theta}}{\partial x} + \frac{\partial \dot{\theta}}{\partial x} \delta \dot{u}_0 \right) + (k_2 B') \left(\dot{v}_0 \frac{\partial \delta \dot{\theta}}{\partial y} + \frac{\partial \dot{\theta}}{\partial y} \delta \dot{v}_0 \right) \right) \\
&\quad + I_2 \left(\frac{\partial \dot{w}_0}{\partial x} \frac{\partial \delta \dot{w}_0}{\partial x} + \frac{\partial \dot{w}_0}{\partial y} \frac{\partial \delta \dot{w}_0}{\partial y} \right) + K_2 \left((k_1 A')^2 \left(\frac{\partial \dot{\theta}}{\partial x} \frac{\partial \delta \dot{\theta}}{\partial x} \right) + (k_2 B')^2 \left(\frac{\partial \dot{\theta}}{\partial y} \frac{\partial \delta \dot{\theta}}{\partial y} \right) \right) \\
&\quad \left. - J_2 \left((k_1 A') \left(\frac{\partial \dot{w}_0}{\partial x} \frac{\partial \delta \dot{\theta}}{\partial x} + \frac{\partial \dot{\theta}}{\partial x} \frac{\partial \delta \dot{w}_0}{\partial x} \right) + (k_2 B') \left(\frac{\partial \dot{w}_0}{\partial y} \frac{\partial \delta \dot{\theta}}{\partial y} + \frac{\partial \dot{\theta}}{\partial y} \frac{\partial \delta \dot{w}_0}{\partial y} \right) \right) \right\} dA
\end{aligned} \tag{50}$$

where dot-superscript convention indicates the differentiation with respect to the time variable t ; $\rho(z)$ is the mass density given by Eq. (1); and (I_i, J_i, K_i) are mass inertias expressed by

$$(I_0, I_1, I_2) = \int_{-h/2}^{h/2} (1, z, z^2) \rho(z) dz \tag{16a}$$

$$(J_1, J_2, K_2) = \int_{-h/2}^{h/2} (f, z f, f^2) \rho(z) dz \tag{16b}$$

By substituting Eqs. (12), (14) and (15) into Eq. (11), the following can be derived

$$\begin{aligned}
\delta u_0 : \quad & \frac{\partial N_x}{\partial x} + \frac{\partial N_{xy}}{\partial y} = I_0 \ddot{u}_0 - I_1 \frac{\partial \ddot{w}_0}{\partial x} + k_1 A' J_1 \frac{\partial \ddot{\theta}}{\partial x} \\
\delta v_0 : \quad & \frac{\partial N_{xy}}{\partial x} + \frac{\partial N_y}{\partial y} = I_0 \ddot{v}_0 - I_1 \frac{\partial \ddot{w}_0}{\partial y} + k_2 B' J_1 \frac{\partial \ddot{\theta}}{\partial y} \\
\delta w_0 : \quad & \frac{\partial^2 M_x^b}{\partial x^2} + 2 \frac{\partial^2 M_{xy}^b}{\partial x \partial y} + \frac{\partial^2 M_y^b}{\partial y^2} + q + N_x^0 \frac{\partial^2 w_0}{\partial x^2} + 2 N_{xy}^0 \frac{\partial^2 w_0}{\partial x \partial y} + N_y^0 \frac{\partial^2 w_0}{\partial y^2} = I_0 \ddot{w}_0 \\
& + I_1 \left(\frac{\partial \ddot{u}_0}{\partial x} + \frac{\partial \ddot{v}_0}{\partial y} \right) - I_2 \nabla^2 \ddot{w}_0 + J_2 \left(k_1 A' \frac{\partial^2 \ddot{\theta}}{\partial x^2} + k_2 B' \frac{\partial^2 \ddot{\theta}}{\partial y^2} \right) \\
\delta \theta : \quad & -k_1 M_x^s - k_2 M_y^s - (k_1 A' + k_2 B') \frac{\partial^2 M_{xy}^s}{\partial x \partial y} + k_1 A' \frac{\partial S_{xz}^s}{\partial x} + k_2 B' \frac{\partial S_{yz}^s}{\partial y} = -J_1 \left(k_1 A' \frac{\partial \ddot{u}_0}{\partial x} + k_2 B' \frac{\partial \ddot{v}_0}{\partial y} \right) \\
& - K_2 \left((k_1 A')^2 \frac{\partial^2 \ddot{\theta}}{\partial x^2} + (k_2 B')^2 \frac{\partial^2 \ddot{\theta}}{\partial y^2} \right) + J_2 \left(k_1 A' \frac{\partial^2 \ddot{w}_0}{\partial x^2} + k_2 B' \frac{\partial^2 \ddot{w}_0}{\partial y^2} \right)
\end{aligned} \tag{17}$$

Substituting Eq. (5) into Eq. (9) and the subsequent results into Eqs. (13), the stress resultants are obtained in terms of strains as following compact form

$$\begin{Bmatrix} N \\ M^b \\ M^s \end{Bmatrix} = \begin{bmatrix} A & B & B^s \\ B & D & D^s \\ B^s & D^s & H^s \end{bmatrix} \begin{Bmatrix} \varepsilon \\ k^b \\ k^s \end{Bmatrix}, \quad S = A^s \gamma, \quad (18)$$

in which

$$N = \{N_x, N_y, N_{xy}\}^t, \quad M^b = \{M_x^b, M_y^b, M_{xy}^b\}^t, \quad M^s = \{M_x^s, M_y^s, M_{xy}^s\}^t, \quad (19a)$$

$$\varepsilon = \{\varepsilon_x^0, \varepsilon_y^0, \gamma_{xy}^0\}^t, \quad k^b = \{k_x^b, k_y^b, k_{xy}^b\}^t, \quad k^s = \{k_x^s, k_y^s, k_{xy}^s\}^t, \quad (19b)$$

$$A = \begin{bmatrix} A_{11} & A_{12} & 0 \\ A_{12} & A_{22} & 0 \\ 0 & 0 & A_{66} \end{bmatrix}, \quad B = \begin{bmatrix} B_{11} & B_{12} & 0 \\ B_{12} & B_{22} & 0 \\ 0 & 0 & B_{66} \end{bmatrix}, \quad D = \begin{bmatrix} D_{11} & D_{12} & 0 \\ D_{12} & D_{22} & 0 \\ 0 & 0 & D_{66} \end{bmatrix}, \quad (19c)$$

$$A = \begin{bmatrix} A_{11} & A_{12} & 0 \\ A_{12} & A_{22} & 0 \\ 0 & 0 & A_{66} \end{bmatrix}, \quad B = \begin{bmatrix} B_{11} & B_{12} & 0 \\ B_{12} & B_{22} & 0 \\ 0 & 0 & B_{66} \end{bmatrix}, \quad D = \begin{bmatrix} D_{11} & D_{12} & 0 \\ D_{12} & D_{22} & 0 \\ 0 & 0 & D_{66} \end{bmatrix}, \quad (19d)$$

$$S = \{S_{xz}^s, S_{yz}^s\}^t, \quad \gamma = \{\gamma_{xz}^0, \gamma_{yz}^0\}^t, \quad A^s = \begin{bmatrix} A_{44}^s & 0 \\ 0 & A_{55}^s \end{bmatrix}, \quad (19e)$$

and stiffness components are given as

$$\begin{Bmatrix} A_{11} & B_{11} & D_{11} & B_{11}^s & D_{11}^s & H_{11}^s \\ A_{12} & B_{12} & D_{12} & B_{12}^s & D_{12}^s & H_{12}^s \\ A_{66} & B_{66} & D_{66} & B_{66}^s & D_{66}^s & H_{66}^s \end{Bmatrix} = \int_{-h/2}^{h/2} C_{11} (1, z, z^2, f(z), z f(z), f^2(z)) \begin{Bmatrix} 1 \\ \nu \\ \frac{1-\nu}{2} \end{Bmatrix} dz, \quad (20a)$$

$$(A_{22}, B_{22}, D_{22}, B_{22}^s, D_{22}^s, H_{22}^s) = (A_{11}, B_{11}, D_{11}, B_{11}^s, D_{11}^s, H_{11}^s), \quad (20b)$$

$$A_{44}^s = A_{55}^s = \int_{-h/2}^{h/2} C_{44} [g(z)]^2 dz, \quad (20c)$$

Introducing Eq. (18) into Eq. (17), the equations of motion can be expressed in terms of displacements (u_0, v_0, w_0, θ) and the appropriate equations take the form

$$\begin{aligned} & A_{11} d_{11} u_0 + A_{66} d_{22} u_0 + (A_{12} + A_{66}) d_{12} v_0 - B_{11} d_{111} w_0 - (B_{12} + 2B_{66}) d_{122} w_0 \\ & + (B_{66}^s (k_1 A^s + k_2 B^s)) d_{122} \theta + (B_{11}^s k_1 + B_{12}^s k_2) d_{11} \theta = I_0 \ddot{u}_0 - I_1 d_1 \dot{w}_0 + J_1 A^s k_1 d_1 \ddot{\theta}, \end{aligned} \quad (21a)$$

$$A_{22} d_{22} v_0 + A_{66} d_{11} v_0 + (A_{12} + A_{66}) d_{12} u_0 - B_{22} d_{222} w_0 - (B_{12} + 2B_{66}) d_{112} w_0 + (B_{66}^s (k_1 A' + k_2 B')) d_{112} \theta + (B_{22}^s k_2 + B_{12}^s k_1) d_2 \theta = I_0 \ddot{v}_0 - I_1 d_2 \ddot{w}_0 + J_1 B' k_2 d_2 \ddot{\theta}, \tag{21b}$$

$$B_{11} d_{111} u_0 + (B_{12} + 2B_{66}) d_{122} u_0 + (B_{12} + 2B_{66}) d_{112} v_0 + B_{22} d_{222} v_0 - D_{11} d_{1111} w_0 - 2(D_{12} + 2D_{66}) d_{1122} w_0 - D_{22} d_{2222} w_0 + (D_{11}^s k_1 + D_{12}^s k_2) d_{11} \theta + 2(D_{66}^s (k_1 A' + k_2 B')) d_{1122} \theta + (D_{12}^s k_1 + D_{22}^s k_2) d_{22} \theta + N_x^0 d_{11} w_0 + 2 N_{xy}^0 d_{12} w_0 + N_y^0 d_{22} w_0 + q = I_0 \ddot{w}_0 + I_1 (d_1 \ddot{u}_0 + d_2 \ddot{v}_0) - I_2 (d_{11} \ddot{w}_0 + d_{22} \ddot{w}_0) + J_2 (k_1 A' d_{11} \ddot{\theta} + k_2 B' d_{22} \ddot{\theta}) \tag{21c}$$

$$- (B_{11}^s k_1 + B_{12}^s k_2) d_1 u_0 - (B_{66}^s (k_1 A' + k_2 B')) d_{122} u_0 - (B_{66}^s (k_1 A' + k_2 B')) d_{112} v_0 - (B_{12}^s k_1 + B_{22}^s k_2) d_2 v_0 + (D_{11}^s k_1 + D_{12}^s k_2) d_{11} w_0 + 2 (D_{66}^s (k_1 A' + k_2 B')) d_{1122} w_0 + (D_{12}^s k_1 + D_{22}^s k_2) d_{22} w_0 - H_{11}^s k_1^2 \theta - H_{22}^s k_2^2 \theta - 2 H_{12}^s k_1 k_2 \theta - ((k_1 A' + k_2 B')^2 H_{66}^s) d_{1122} \theta + A_{44}^s (k_2 B')^2 d_{22} \theta + A_{55}^s (k_1 A')^2 d_{11} \theta = -J_1 (k_1 A' d_1 \ddot{u}_0 + k_2 B' d_2 \ddot{v}_0) + J_2 (k_1 A' d_{11} \ddot{w}_0 + k_2 B' d_{22} \ddot{w}_0) - K_2 ((k_1 A')^2 d_{11} \ddot{\theta} + (k_2 B')^2 d_{22} \ddot{\theta}) \tag{21d}$$

where d_{ij} , d_{ijl} and d_{ijlm} are the following differential operators

$$d_{ij} = \frac{\partial^2}{\partial x_i \partial x_j}, \quad d_{ijl} = \frac{\partial^3}{\partial x_i \partial x_j \partial x_l}, \quad d_{ijlm} = \frac{\partial^4}{\partial x_i \partial x_j \partial x_l \partial x_m}, \quad d_i = \frac{\partial}{\partial x_i}, \quad (i, j, l, m = 1, 2). \tag{22}$$

2.3 Analytical solution for simply-supported FG plates

The Navier solution method is employed to determine the analytical solutions for which the displacement variables are written as product of arbitrary parameters and known trigonometric functions to respect the equations of motion and boundary conditions

$$\begin{Bmatrix} u_0 \\ v_0 \\ w_0 \\ \theta \end{Bmatrix} = \sum_{m=1}^{\infty} \sum_{n=1}^{\infty} \begin{Bmatrix} U_{mn} e^{i\omega t} \cos(\alpha x) \sin(\beta y) \\ V_{mn} e^{i\omega t} \sin(\alpha x) \cos(\beta y) \\ W_{mn} e^{i\omega t} \sin(\alpha x) \sin(\beta y) \\ X_{mn} e^{i\omega t} \sin(\alpha x) \sin(\beta y) \end{Bmatrix} \tag{23}$$

where ω is the frequency of free vibration of the plate, $\sqrt{-1}$ the imaginary unit. with

$$\alpha = m\pi / a \quad \text{and} \quad \beta = n\pi / b \tag{24}$$

The transverse load q is also expanded in the double-Fourier sine series as

$$q(x, y) = \sum_{m=1}^{\infty} \sum_{n=1}^{\infty} Q_{mn} \sin(\alpha x) \sin(\beta y), \tag{25}$$

where

$$Q_{mn} = \frac{4}{ab} \int_0^a \int_0^b q(x, y) \sin(\alpha x) \sin(\beta y) dx dy = \begin{cases} q_0 & \text{for sinusoidally distributed load} \\ \frac{16q_0}{mn\pi^2} & \text{for uniformly distributed load} \end{cases} \quad (26)$$

Considering that the plate is subjected to in-plane compressive loads of form: $N_x^0 = \gamma_1 N_{cr}$, $N_y^0 = \gamma_2 N_{cr}$, $N_{xy}^0 = 0$ (here γ_1 and γ_2 are non-dimensional load parameters).

Substituting Eq. (23) into Eq. (22), the following problem is obtained

$$\left(\begin{bmatrix} S_{11} & S_{12} & S_{13} & S_{14} \\ S_{12} & S_{22} & S_{23} & S_{24} \\ S_{13} & S_{23} & S_{33}+k & S_{34} \\ S_{14} & S_{24} & S_{34} & S_{44} \end{bmatrix} - \omega^2 \begin{bmatrix} m_{11} & 0 & m_{13} & m_{14} \\ 0 & m_{22} & m_{23} & m_{24} \\ m_{13} & m_{23} & m_{33} & m_{34} \\ m_{14} & m_{24} & m_{34} & m_{44} \end{bmatrix} \right) \begin{Bmatrix} U_{mn} \\ V_{mn} \\ W_{mn} \\ X_{mn} \end{Bmatrix} = \begin{Bmatrix} 0 \\ 0 \\ Q_{mn} \\ 0 \end{Bmatrix} \quad (27)$$

where

$$\begin{aligned} S_{11} &= -(A_{11}\alpha^2 + A_{66}\beta^2), & S_{12} &= -\alpha\beta (A_{12} + A_{66}), \\ S_{13} &= \alpha(B_{11}\alpha^2 + B_{12}\beta^2 + 2B_{66}\beta^2), & S_{14} &= \alpha(k_1 B_{11}^s + k_2 B_{12}^s - (k_1 A' + k_2 B') B_{66}^s \alpha^2), \\ S_{22} &= -(A_{66}\alpha^2 + A_{22}\beta^2), & S_{23} &= \beta(B_{22}\beta^2 + B_{12}\alpha^2 + 2B_{66}\alpha^2), \\ S_{24} &= \beta(k_2 B_{22}^s + k_1 B_{12}^s - (k_1 A' + k_2 B') B_{66}^s \alpha^2), & S_{33} &= -(D_{11}\alpha^4 + 2(D_{12} + 2D_{66})\alpha^2\beta^2 + D_{22}\beta^4), \\ S_{34} &= -k_1(D_{11}^s\alpha^2 + D_{12}^s\beta^2) + 2(k_1 A' + k_2 B') D_{66}^s \alpha^2\beta^2 - k_2(D_{22}^s\beta^2 + D_{12}^s\alpha^2), \\ S_{44} &= -k_1(H_{11}^s k_1 + H_{12}^s k_2) - (k_1 A' + k_2 B')^2 H_{66}^s \alpha^2\beta^2 - k_2(H_{12}^s k_1 + H_{22}^s k_2) \\ &\quad - (k_1 A')^2 A_{55}^s \alpha^2 - (k_2 B')^2 A_{44}^s \beta^2, & k &= N_{cr} (\gamma_1 \alpha^2 + \gamma_2 \beta^2) \end{aligned} \quad (28)$$

$$m_{11} = -I_0, \quad m_{13} = \alpha I_1, \quad m_{14} = -J_1 k_1 A' \alpha, \quad m_{22} = -I_0, \quad m_{23} = \beta I_1, \quad m_{24} = -k_2 B' \beta J_1,$$

$$m_{33} = -I_0 - I_2 (\alpha^2 + \beta^2), \quad m_{34} = J_2 (k_1 A' \alpha^2 + k_2 B' \beta^2), \quad m_{44} = -K_2 ((k_1 A')^2 \alpha^2 + (k_2 B')^2 \beta^2)$$

3. Numerical examples and discussions

In this section, various numerical examples are presented and discussed to check the accuracy of present HSDT in investigating the bending, buckling, and vibration behaviors of simply supported FG plates. For proposed examples, an Al/Al₂O₃ plate fabricated of aluminum (as metal) and alumina (as ceramic) is examined. The Young's modulus and density of aluminum are $E_m = 70$ GPa and $\rho_m = 2702$ kg/m³, respectively, and those of alumina are $E_c = 380$ GPa and $\rho_c = 3800$ kg/m³, respectively. For validation purpose, the computed quantities are compared with those reported utilizing various existing plate models. The description of various plate theories is illustrated in Table 1. In all examples, a shear correction coefficient of 5/6 is employed for FSDT

Table 1 Displacement models

Model	Theory	Unknowns
CPT	Classical plate theory	3
FSDT	First-order shear deformation theory	5
TSDT	Third-order shear deformation theory	5
HySDT	Hyperbolic shear deformation theory	5
SSDT	Sinusoidal shear deformation theory	5
Present	New higher shear deformation theory	4

and the rotary inertias are incorporated in all models. The Poisson's ratio of the plate is considered to be constant across the thickness and equal to 0.3. For convenience, the following dimensionless quantities are employed in illustrating the numerical results in graphical and tabular form

$$\begin{aligned}
 \bar{w} &= \frac{10 E_c h^3}{q_0 a^4} w \left(\frac{a}{2}, \frac{b}{2} \right), & \bar{\sigma}_x &= \frac{h}{q_0 a} \sigma_x \left(\frac{a}{2}, \frac{b}{2}, \frac{h}{2} \right), & \bar{\sigma}_y &= \frac{h}{q_0 a} \sigma_y \left(\frac{a}{2}, \frac{b}{2}, \frac{h}{3} \right), \\
 \bar{\tau}_{xy} &= \frac{h}{q_0 a} \tau_{xy} \left(0, 0, -\frac{h}{3} \right), & \bar{\tau}_{xz} &= \frac{h}{q_0 a} \tau_{xz} \left(0, \frac{b}{2}, 0 \right), & \bar{\tau}_{yz} &= \frac{h}{q_0 a} \tau_{yz} \left(\frac{a}{2}, 0, \frac{h}{6} \right), \\
 D &= \frac{E h^3}{12(1-\nu^2)}, & \hat{N} &= \frac{N_{cr} b^2}{\pi^2 D}, & \bar{N} &= \frac{N_{cr} a^2}{E_m h^3}, & \hat{\omega} &= \omega h \sqrt{\rho_c / E_c}, & \bar{\omega} &= \omega \frac{a^2}{h} \sqrt{\rho_c / E_c}
 \end{aligned} \quad (29)$$

3.1 Bending problem

Example 1: Table 2 presents the comparison of non-dimensional transverse displacements and stresses of square FG plate subjected to uniformly distributed load ($a/h = 10$). The computed results are compared with those reported by Zenkour (2006) based on sinusoidal shear deformation theory (SSDT). It can be observed that a good agreement is demonstrated for all values of power law exponent p . It should be signaled that the developed novel HSDT involves four variables as against five in case of SSDT (Zenkour 2006).

Example 2: The second example is performed for square FG plate subjected to sinusoidally distributed load ($a/h = 10$). In Table 3 the comparison of non-dimensional deflections and stresses determined by present model with those provided by Benyoucef *et al.* (2010) based on the hyperbolic shear deformation theory (HySDT) is carried out. It can be confirmed that an excellent agreement is proved for all values of power law exponent p . It is remarked that the stresses for a fully ceramic plate are identical to those for a fully metal plate. This is due to the fact that the structure for these two cases is fully homogenous and the non-dimensional stresses are not related to the value of the elastic modulus.

To demonstrate the validity of the present model for large range of power law exponent and thickness ratio a/h , the variations of non-dimensional transverse displacement \bar{w} as a function of the power law index p and thickness ratio a/h are shown in Figs. 1 and 2 respectively, for square FG plate under sinusoidally distributed load. The curves determined from the proposed model are compared with the curves determined of the CPT and the TSDT developed by Reddy (2000).

Table 2 Comparison of non-dimensional deflection and stresses of square plate under uniformly distributed load ($m, n = 100$ term series, $a = 10$ h)

p	Method	\bar{w}	$\bar{\sigma}_x$	$\bar{\sigma}_y$	$\bar{\tau}_{xy}$	$\bar{\tau}_{yz}$	$\bar{\tau}_{xz}$
Ceramic	SSDT ^(a)	0.4665	2.8932	1.9103	1.2850	0.4429	0.5114
	Present	0.4666	2.8917	1.9107	1.2850	0.4422	0.4975
1	SSDT ^(a)	0.9287	4.4745	2.1962	1.1143	0.5446	0.5114
	Present	0.9288	4.4720	2.1697	1.1143	0.5437	0.4975
2	SSDT ^(a)	1.1940	5.2296	2.0338	0.9907	0.5734	0.4700
	Present	1.1940	5.2262	2.0345	0.9909	0.5700	0.4552
3	SSDT ^(a)	1.3200	5.6108	1.8593	1.0047	0.5629	0.4367
	Present	1.3197	5.6066	1.8603	1.0050	0.5570	0.4211
4	SSDT ^(a)	1.3890	5.8915	1.7197	1.0298	0.5346	0.4204
	Present	1.3884	5.8868	1.7209	1.0302	0.5276	0.4042
5	SSDT ^(a)	1.4356	6.1504	1.6104	1.0451	0.5031	0.4177
	Present	1.4349	6.1454	1.6117	1.0456	0.4959	0.4011
6	SSDT ^(a)	1.4727	6.4043	1.5214	1.0536	0.4755	0.4227
	Present	1.4719	6.3991	1.5227	1.0541	0.4688	0.4060
7	SSDT ^(a)	1.5049	6.6547	1.4467	1.0589	0.4543	0.4310
	Present	1.5042	6.6494	1.4479	1.0593	0.4483	0.4143
8	SSDT ^(a)	1.5343	6.8999	1.3829	1.0628	0.4392	0.4399
	Present	1.5337	6.8946	1.3841	1.0632	0.4339	0.4234
9	SSDT ^(a)	1.5617	7.1883	1.3283	1.0620	0.4291	0.4481
	Present	1.5612	7.1332	1.3295	1.0666	0.4245	0.4319
10	SSDT ^(a)	1.5876	7.3689	1.2820	1.0694	0.4227	0.4542
	Present	1.5872	7.3638	1.2831	1.0698	0.4187	0.4393
Metal	SSDT ^(a)	2.5327	2.8932	1.9103	1.2850	0.4429	0.5114
	Present	2.5329	2.8917	1.9106	1.2850	0.4422	0.4975

^(a) Taken from Zenkour (2006)

Table 3 Comparison of non-dimensional deflection and stresses of square plate under sinusoidally distributed load ($a = 10$ h)

p	Method	\bar{w}	$\bar{\sigma}_x$	$\bar{\sigma}_y$	$\bar{\tau}_{xy}$	$\bar{\tau}_{yz}$	$\bar{\tau}_{xz}$
Ceramic	HySDT ^(a)	0.2960	1.9955	1.3121	0.7065	0.2132	0.2462
	Present	0.2960	1.9943	1.3124	0.7067	0.2121	0.2386
1	HySDT ^(a)	0.5889	3.0870	1.4894	0.6110	0.2622	0.2462
	Present	0.5889	3.0850	1.4898	0.6111	0.2608	0.2386
2	HySDT ^(a)	0.7573	3.6094	1.3954	0.5441	0.2763	0.2265
	Present	0.7573	3.6067	1.3960	0.5442	0.2737	0.2186

Table 3 Continued

p	Method	\bar{w}	$\bar{\sigma}_x$	$\bar{\sigma}_y$	$\bar{\tau}_{xy}$	$\bar{\tau}_{yz}$	$\bar{\tau}_{xz}$
3	HySDT ^(a)	0.8377	3.8742	1.2748	0.5525	0.2715	0.2107
	Present	0.8375	3.8709	1.2756	0.5526	0.2677	0.2024
4	HySDT ^(a)	0.8819	4.0693	1.1783	0.5667	0.2580	0.2029
	Present	0.8815	4.0655	1.1794	0.5669	0.2537	0.1944
5	HySDT ^(a)	0.9118	4.2488	1.1029	0.5755	0.2429	0.2017
	Present	0.9114	4.2447	1.1041	0.5758	0.2385	0.1930
6	HySDT ^(a)	0.9356	4.4244	1.0417	0.5803	0.2296	0.2041
	Present	0.9351	4.4201	1.0428	0.5806	0.2256	0.1954
7	HySDT ^(a)	0.9562	4.5971	0.9903	0.5834	0.2194	0.2081
	Present	0.9558	4.5928	0.9915	0.5836	0.2157	0.1994
8	HySDT ^(a)	0.9750	4.7661	0.9466	0.5856	0.2121	0.2124
	Present	0.9746	4.7619	0.9477	0.5858	0.2088	0.2037
9	HySDT ^(a)	0.9925	4.9303	0.9092	0.5875	0.2072	0.2164
	Present	0.9921	4.9261	0.9103	0.5878	0.2042	0.2078
10	HySDT ^(a)	1.0089	5.0890	0.8775	0.5894	0.2041	0.2198
	Present	1.0087	5.0849	0.8785	0.5896	0.2014	0.2114
Metal	HySDT ^(a)	1.6070	1.9955	1.3121	0.7065	0.2132	0.2462
	Present	1.6072	1.9943	1.3124	0.7067	0.2121	0.2386

^(a) Taken from Benyoucef *et al.* (2010)

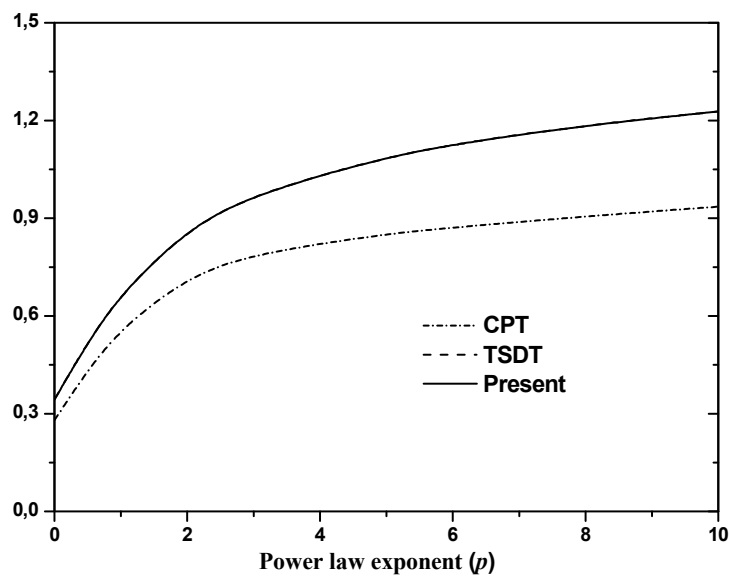


Fig. 1 Comparison of the variation of non-dimensional deflection \bar{w} of square FG plate under sinusoidally distributed load versus power law index p ($a/h = 5$)

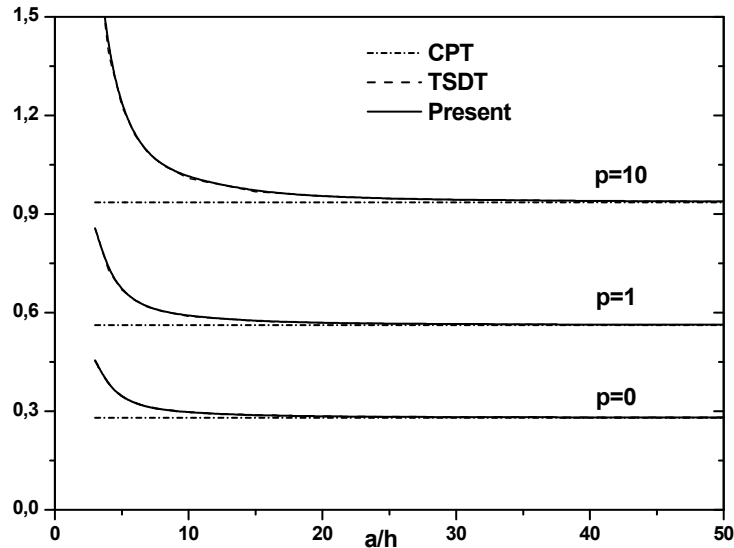


Fig. 2 Comparison of the variation of non-dimensional deflection \bar{w} of square FG plate under sinusoidally distributed load versus thickness ratio a/h

It can be observed that the curves of present model and TSDT are almost identical, and the CPT underestimates the transverse displacement of plate. Since the transverse shear deformation influences are not included in CPT, the values of non-dimensional transverse displacement \bar{w} computed by CPT are not affected by the variation of thickness ratio a/h (see Fig. 2). Thus, in general, the present model is successfully checked.

3.2 Buckling problem

Example 3: Table 4 presents the values of the non-dimensional buckling loads \hat{N} of isotropic plate ($p = 0$) under various loading cases for various values of aspect ratio a/b and thickness ratio h/b . The computed values are compared with the results reported by Shufrin and Eisenberger (2005) based on FSDT and TSDT. An excellent agreement is proved for all types ranging from moderately thick to very thick plates.

Table 4 Comparison of non-dimensional critical buckling load \hat{N} of isotropic plate under different loading types ($p = 0$)

a/b	h/b	Method	Loading type (γ_1, γ_2)		
			(1,0)	(0,1)	(1,1)
1	0.1	FSDT ^(a)	3.7865	3.7865	1.8932
		TSDT ^(a)	3.7866	3.7865	1.8933
		Present	3.7866	3.7865	1.8933
	0.2	FSDT ^(a)	3.2638	3.2637	1.6319
		TSDT ^(a)	3.2653	3.2653	1.6327
		Present	3.2653	3.2653	1.6327

Table 4 Continued

a/b	h/b	Method	Loading type (γ_1, γ_2)		
			(1,0)	(0,1)	(1,1)
1	0.3	FSDT ^(a)	2.6533	2.6533	1.3266
		TSDT ^(a)	2.6586	2.6586	1.3293
		Present	2.6586	2.6586	1.3293
	0.4	FSDT ^(a)	1.9196	1.9196	1.0513
		TSDT ^(a)	1.9550	1.9550	1.0567
		Present	1.9550	1.9550	1.0567
1.5	0.1	FSDT ^(a)	4.0250	2.0048	1.3879
		TSDT ^(a)	4.0253	2.0048	1.3879
		Present	4.0253	2.0048	1.3879
	0.2	FSDT ^(a)	3.3048	1.7941	1.2421
		TSDT ^(a)	3.3077	1.7946	1.2424
		Present	3.3077	1.7946	1.2424
	0.3	FSDT ^(a)	2.5457	1.5267	1.0570
		TSDT ^(a)	2.5545	1.5285	1.0582
		Present	2.5545	1.5285	1.0582
	0.4	FSDT ^(a)	1.9196	1.2632	0.8745
		TSDT ^(a)	1.9421	1.2670	0.8772
		Present	1.9421	1.2670	0.8772
2	0.1	FSDT ^(a)	3.7865	1.5093	1.2074
		TSDT ^(a)	3.7866	1.5093	1.2075
		Present	3.7866	1.5093	1.2074
	0.2	FSDT ^(a)	3.2637	1.3694	1.0955
		TSDT ^(a)	3.2654	1.3697	1.0958
		Present	3.2654	1.3697	1.0958
	0.3	FSDT ^(a)	2.5726	1.1862	0.9490
		TSDT ^(a)	2.5839	1.1873	0.9498
		Present	2.6539 ^c	1.1873	0.9498
	0.4	FSDT ^(a)	1.9034	0.9991	0.7992
		TSDT ^(a)	1.9230	1.0015	0.8012
		Present	1.9230 ^c	1.0015	0.8012

^(a) Taken from Shufrin and Eisenberger (2005)

Figs. 3 and 4 present the variations of non-dimensional critical buckling load \bar{N} as a function of the power law exponent p and thickness ratio a/h , respectively, for square FG plate under biaxial compression. It is demonstrated that the present novel four variable refined plate theory and TSDT predict almost the same values, and CPT over-estimates the buckling loads of plate due to

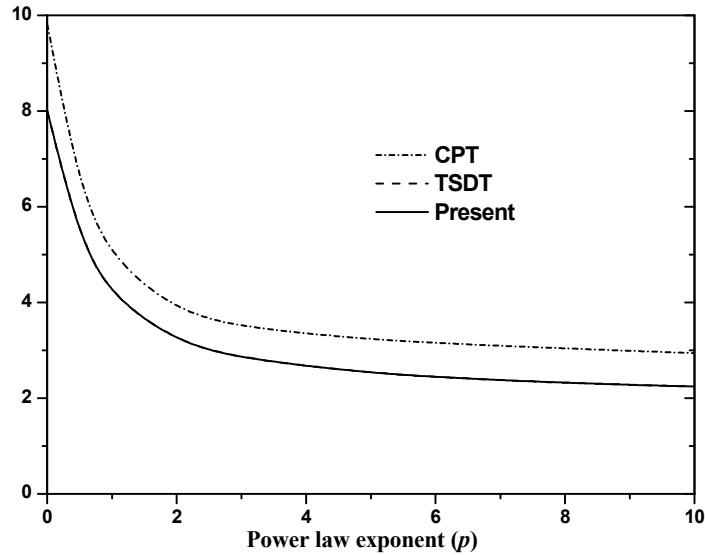


Fig. 3 Comparison of the variation of non-dimensional critical buckling load \bar{N} of square FG plate under biaxial compression versus power law exponent p ($a/h = 5$)

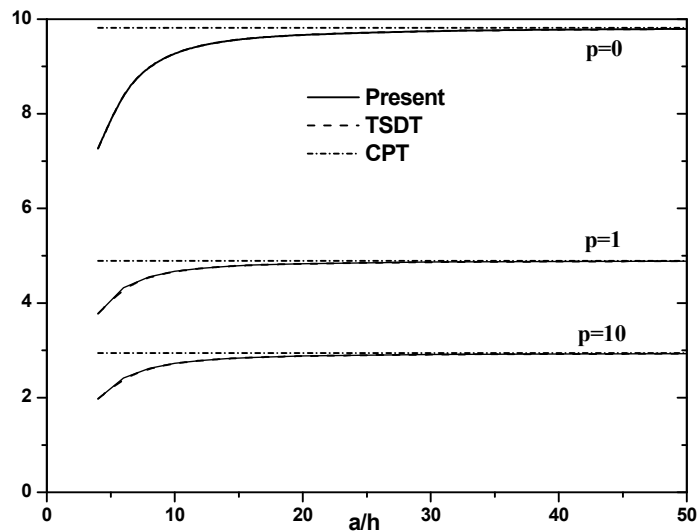


Fig. 4 Comparison of the variation of non-dimensional critical buckling load \bar{N} of square plate under biaxial compression versus thickness ratio a/h

neglecting transverse shear deformation influences. The difference between CPT and shear deformation models diminishes when the side-to-thickness ratio a/h increases (see Fig. 4).

3.3 Free vibration problem

Example 4: Table 5 presents the results of non-dimensional fundamental frequencies $\hat{\omega}$ of square FG plate for various values of thickness ratio h/a and power law exponent p . The

computed data are compared with those calculated by and Hosseini-Hashemi *et al.* (2011a) based on FSDT and and Hosseini-Hashemi *et al.* (2011b) based on TSDT. It is concluded from Table 5 that there is an excellent agreement between the results determined by present model, FSDT (Hosseini-Hashemi *et al.* 2011a), and TSDT (Hosseini-Hashemi *et al.* 2011b).

Example 5: The comparison presented in Table 6 is performed to check the higher order modes of vibration. For this end, the first four non-dimensional frequencies $\bar{\omega}$ are given in Table 6 for rectangular FG plate ($b = 2a$) with different values of thickness ratio and power law exponent. The non-dimensional frequencies determined by employing the developed model and TSDT (2000) are compared with those reported by Hosseini-Hashemi *et al.* (2011a) based on FSDT. It is remarked that there is a good agreement between the values computed by the present model, FSDT (Hosseini-Hashemi *et al.* 2011a), and TSDT for all modes of vibration of thin to thick plates.

Table 5 Comparison of non-dimensional fundamental frequency $\hat{\omega}$ of FG plate

a/h	Method	Power law exponent (p)				
		0	0.5	1	4	10
5	FSDT ^(a)	0.2112	0.1805	0.1631	0.1397	0.1324
	HSDT ^(b)	0.2113	0.1807	0.1631	0.1378	0.1301
	Present	0.2113	0.1807	0.1631	0.1378	0.1301
10	FSDT ^(a)	0.0577	0.0490	0.0442	0.0382	0.0366
	HSDT ^(b)	0.0577	0.0490	0.0442	0.0381	0.0364
	Present	0.0577	0.0490	0.0442	0.0381	0.0364
20	FSDT ^(a)	0.0148	0.0125	0.0113	0.0098	0.0094
	HSDT ^(b)	0.0148	0.0125	0.0113	0.0098	0.0094
	Present	0.0148	0.0125	0.0113	0.0098	0.0094

^(a) Taken from Hosseini-Hashemi *et al.* (2011a)

^(b) Taken from Hosseini-Hashemi *et al.* (2011b)

Table 6 Comparison of the first four non-dimensional fundamental frequencies $\bar{\omega}$ of rectangular FG plate ($b = 2a$)

a/h	Mode (m, n)	Method	Power law exponent (p)						
			0	0.5	1	2	5	8	10
1	(1,1)	FSDT ^(a)	3.4409	2.9322	2.6473	2.4017	2.2528	2.1985	2.1677
		TSDT	3.4412	2.9347	2.6475	2.3949	2.2272	2.1697	2.1407
		Present	3.4412	2.9347	2.6475	2.3949	2.2272	2.1697	2.1407
5	2 (1,2)	FSDT ^(a)	5.2802	4.5122	4.0773	3.6953	3.4492	3.3587	3.3094
		TSDT	5.2813	4.5180	4.0781	3.6805	3.3938	3.2964	3.2514
		Present	5.2813	4.5180	4.0781	3.6805	3.3938	3.2964	3.2514
3	(1,3)	FSDT ^(a)	8.0710	6.9231	6.2636	5.6695	5.2579	5.1045	5.0253
		TSDT	8.0749	6.9366	6.2663	5.6390	5.1425	4.9758	4.9055
		Present	8.0749	6.9366	6.2663	5.6390	5.1425	4.9758	4.9055

Table 6 Continued

a/h	Mode (m, n)	Method	Power law exponent (p)						
			0	0.5	1	2	5	8	10
5	4 (2,1)	FSDT ^(a)	9.7416	8.6926	7.8711	7.1189	6.5749	5.9062	5.7518
		TSDT	10.1164	8.7138	7.8762	7.0751	6.4074	6.1846	6.0954
		Present	10.1164	8.7138	7.8762	7.0751	6.4074	6.1846	6.0954
10	1 (1,1)	FSDT ^(a)	3.6518	3.0983	2.7937	2.5386	2.3998	2.3504	2.3197
		TSDT	3.6518	3.0990	2.7937	2.5364	2.3916	2.3411	2.3110
		Present	3.6518	3.0990	2.7937	2.5364	2.3916	2.3411	2.3110
	2 (1,2)	FSDT ^(a)	5.7693	4.8997	4.4192	4.0142	3.7881	3.7072	3.6580
		TSDT	5.7694	4.9014	4.4192	4.0090	3.7682	3.6846	3.6368
		Present	5.7694	4.9014	4.4192	4.0090	3.7682	3.6846	3.6368
	3 (1,3)	FSDT ^(a)	9.1876	7.8145	7.0512	6.4015	6.0247	5.8887	5.8086
		TSDT	9.1887	7.8189	7.0515	6.3886	5.9765	5.8341	5.7575
		Present	9.1887	7.8189	7.0515	6.3886	5.9765	5.8341	5.7575
	4 (2,1)	FSDT ^(a)	11.8310	10.0740	9.0928	8.2515	7.7505	7.5688	7.4639
		TSDT	11.8315	10.0810	9.0933	8.2309	7.6731	7.4813	7.3821
		Present	11.8315	10.0810	9.0933	8.2309	7.6731	7.4813	7.3821
20	1 (1,1)	FSDT ^(a)	3.7123	3.1456	2.8352	2.5777	2.4425	2.3948	2.3642
		TSDT	3.7123	3.1458	2.8352	2.5771	2.4403	2.3923	2.3619
		Present	3.7123	3.1458	2.8352	2.5771	2.4403	2.3923	2.3619
	2 (1,2)	FSDT ^(a)	5.9198	5.0175	4.5228	4.1115	3.8939	3.8170	3.7681
		TSDT	5.9199	5.0180	4.5228	4.1100	3.8884	3.8107	3.7622
		Present	5.9199	5.0180	4.5228	4.1100	3.8884	3.8107	3.7622
	3 (1,3)	FSDT ^(a)	9.5668	8.1121	7.3132	6.6471	6.2903	6.1639	6.0843
		TSDT	9.5669	8.1133	7.3132	6.6433	6.2760	6.1476	6.0690
		Present	9.5669	8.1133	7.3132	6.6433	6.2760	6.1476	6.0690
	4 (2,1)	FSDT ^(a)	12.4560	10.5660	9.5261	8.6572	8.1875	8.0207	7.9166
		TSDT	12.4562	10.5677	9.5261	8.6509	8.1636	7.9934	7.8909
		Present	12.4562	10.5677	9.5261	8.6509	8.1636	7.9934	7.8909

^(a) Taken from Hosseini-Hashemi *et al.* (2011a)

The variations of non-dimensional fundamental frequency $\bar{\omega}$ of square FG plate as a function of the power law exponent p and thickness ratio a/h are presented in Figs. 5 and 6, respectively. The curves plotted by using the present theory are compared with the curves plotted by employing the CPT and the TSDT (Reddy 2000). From this investigation can be observed that the resulting curves are very close to the curves plotted by employing a TSDT (Reddy 2000) and the CPT overestimates the results of thick plate. Thus, in general, the present model is successfully validated.

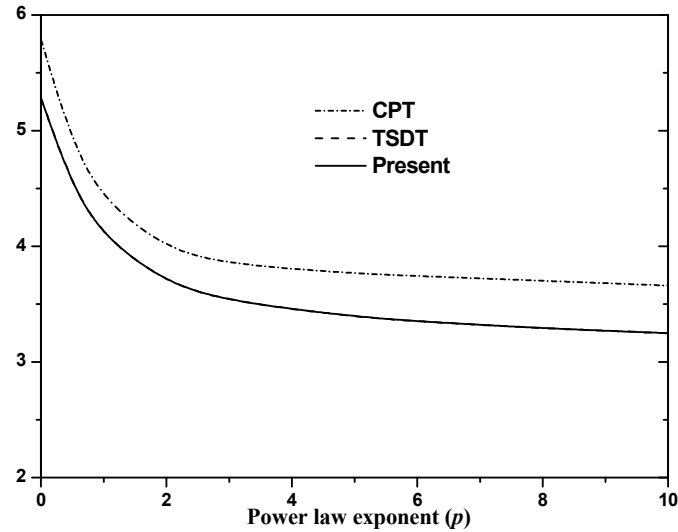


Fig. 5 Comparison of the variation of non-dimensional fundamental frequency $\bar{\omega}$ of square FG plate versus power law index p ($a/h = 5$)

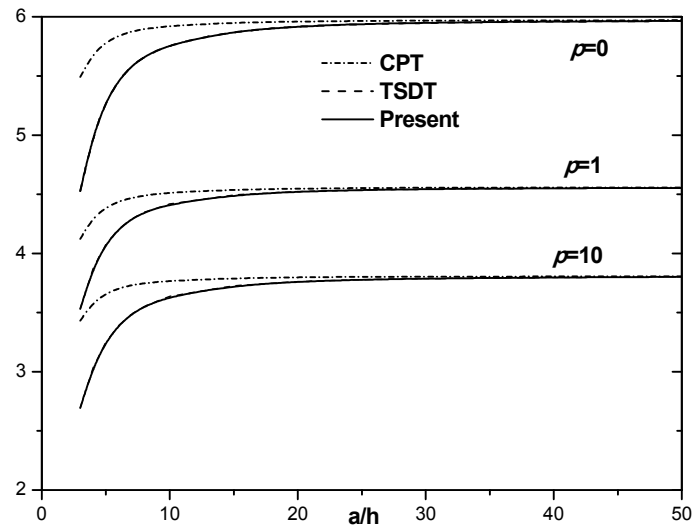


Fig. 6 Comparison of the variation of non-dimensional fundamental frequency $\bar{\omega}$ of square FG plate versus thickness ratio a/h

4. Conclusions

A novel higher-order shear deformation theory is developed for bending, buckling, and vibration of FG plates. By considering further simplifying suppositions to the existing HSDT, with the incorporation of an undetermined integral term, the number of variables and equations of motion of the present HSDT are diminished by one, and hence, make this model simple and efficient to employ. The equations of motion are determined by utilizing the Hamilton's principle

and then are solved using Navier's procedure. The exactitude of the developed model has been checked for the bending, buckling, and free vibration responses of FG plates. All comparison investigations demonstrate that the deflection, stress, buckling load, and natural frequency determined by the developed model with four variables are almost close to those obtained by other shear deformation theories containing five variables. In conclusion, it can be deduced from this work that the developed theory is accurate and efficient in investigating the bending, buckling, and vibration behaviors of FG plates.

References

- Ait Amar Meziane, M., Abdelaziz, H.H. and Tounsi, A. (2014), "An efficient and simple refined theory for buckling and free vibration of exponentially graded sandwich plates under various boundary conditions", *J. Sandw. Struct. Mater.*, **16**(3), 293-318.
- Ait Atmane, H., Tounsi, A., Bernard, F. and Mahmoud, S.R. (2015), "A computational shear displacement model for vibrational analysis of functionally graded beams with porosities", *Steel Compos. Struct., Int. J.*, **19**(2), 369-384.
- Ait Yahia, S., Ait Atmane, H., Houari, M.S.A. and Tounsi, A. (2015), "Wave propagation in functionally graded plates with porosities using various higher-order shear deformation plate theories", *Struct. Eng. Mech., Int. J.*, **53**(6), 1143-1165.
- Akavci, S.S. (2015), "An efficient shear deformation theory for free vibration of functionally graded thick rectangular plates on elastic foundation", *Compos. Struct.*, **108**, 667-676.
- Akbaş, Ş.D. (2015), "Wave propagation of a functionally graded beam in thermal environments", *Steel Compos. Struct., Int. J.*, **19**(6), 1421-1447.
- Al-Basyouni, K.S., Tounsi, A. and Mahmoud, S.R. (2015), "Size dependent bending and vibration analysis of functionally graded micro beams based on modified couple stress theory and neutral surface position", *Compos. Struct.*, **125**, 621-630.
- Arefi, M. (2015), "Elastic solution of a curved beam made of functionally graded materials with different cross sections", *Steel Compos. Struct., Int. J.*, **18**(3), 659-672.
- Attia, A., Tounsi, A., Adda Bedia, E.A. and Mahmoud, S.R. (2015), "Free vibration analysis of functionally graded plates with temperature-dependent properties using various four variable refined plate theories", *Steel Compos. Struct., Int. J.*, **18**(1), 187-212.
- Bakora, A. and Tounsi, A. (2015), "Thermo-mechanical post-buckling behavior of thick functionally graded plates resting on elastic foundations", *Struct. Eng. Mech., Int. J.*, **56**(1), 85-106.
- Belabed, Z., Houari, M.S.A., Tounsi, A., Mahmoud, S.R. and Anwar Bég, O. (2014), "An efficient and simple higher order shear and normal deformation theory for functionally graded material (FGM) plates", *Composites: Part B*, **60**, 274-283.
- Beldjelili, Y., Tounsi, A. and Mahmoud, S.R. (2016), "Hygro-thermo-mechanical bending of S-FGM plates resting on variable elastic foundations using a four-variable trigonometric plate theory", *Smart Struct. Syst., Int. J.*, **18**(4), 755-786.
- Bellifa, H., Benrahou, K.H., Hadji, L., Houari, M.S.A. and Tounsi, A. (2016), "Bending and free vibration analysis of functionally graded plates using a simple shear deformation theory and the concept the neutral surface position", *J. Braz. Soc. Mech. Sci. Eng.*, **38**(1), 265-275.
- Belkorissat, I., Houari, M.S.A., Tounsi, A., Adda Bedia, E.A. and Mahmoud, S.R. (2015), "On vibration properties of functionally graded nano-plate using a new nonlocal refined four variable model", *Steel Compos. Struct., Int. J.*, **18**(4), 1063-1081.
- Bennai, R., Ait Atmane, H. and Tounsi, A. (2015), "A new higher-order shear and normal deformation theory for functionally graded sandwich beams", *Steel Compos. Struct., Int. J.*, **19**(3), 521-546.
- Bennoun, M., Houari, M.S.A. and Tounsi, A. (2016), "A novel five variable refined plate theory for vibration analysis of functionally graded sandwich plates", *Mech. Adv. Mater. Struct.*, **23**(4), 423-431.

- Benyoucef, S., Mechab, I., Tounsi, A., Fekrar, A., Ait Atmane, H. and Adda Bedia, E.A. (2010), "Bending of thick functionally graded plates resting on Winkler–Pasternak elastic foundations", *Mech. Compos. Mater.*, **46**(4), 425-434.
- Bouchafa, A., Bachir Bouiadjra, M., Houari, M.S.A. and Tounsi, A. (2015), "Thermal stresses and deflections of functionally graded sandwich plates using a new refined hyperbolic shear deformation theory", *Steel Compos. Struct., Int. J.*, **18**(6), 1493-1515.
- Bouderba, B., Houari, M.S.A. and Tounsi, A. (2013), "Thermomechanical bending response of FGM thick plates resting on Winkler–Pasternak elastic foundations", *Steel Compos. Struct., Int. J.*, **14**(1), 85-104.
- Bouderba, B., Houari, M.S.A. and Tounsi, A. and Mahmoud, S.R. (2016), "Thermal stability of functionally graded sandwich plates using a simple shear deformation theory", *Struct. Eng. Mech., Int. J.*, **58**(3), 397-422.
- Bouguenina, O., Belakhdar, K., Tounsi, A. and Adda Bedia, E.A. (2015), "Numerical analysis of FGM plates with variable thickness subjected to thermal buckling", *Steel Compos. Struct., Int. J.*, **19**(3), 679-695.
- Boukhari, A., Ait Atmane, H., Tounsi, A., Adda Bedia, E.A. and Mahmoud, S.R. (2016), "An efficient shear deformation theory for wave propagation of functionally graded material plates", *Struct. Eng. Mech., Int. J.*, **57**(5), 837-859.
- Bounouara, F., Benrahou, K.H., Belkorissat, I. and Tounsi, A. (2016), "A nonlocal zeroth-order shear deformation theory for free vibration of functionally graded nanoscale plates resting on elastic foundation", *Steel Compos. Struct., Int. J.*, **20**(2), 227-249.
- Bourada, M., Kaci, A., Houari, M.S.A., Tounsi, A. (2015), "A new simple shear and normal deformations theory for functionally graded beams", *Steel Compos. Struct., Int. J.*, **18**(2), 409-423.
- Bourada, F., Amara, K., Tounsi, A. (2016), "Buckling analysis of isotropic and orthotropic plates using a novel four variable refined plate theory", *Steel Compos. Struct., Int. J.*, **21**(6), 1287-1306.
- Bousahla, A.A., Houari, M.S.A., Tounsi, A. and Adda Bedia, E.A. (2014), "A novel higher order shear and normal deformation theory based on neutral surface position for bending analysis of advanced composite plates", *Int. J. Computat. Method.*, **11**(6), 1350082.
- Bousahla, A.A., Benyoucef, S. Tounsi, A. and Mahmoud, S.R. (2016), "On thermal stability of plates with functionally graded coefficient of thermal expansion", *Struct. Eng. Mech., Int. J.*, **60**(2), 313-335.
- Carrera, E., Brischetto, S., Cinefra, M. and Soave, M. (2010), "Refined and advanced models for multilayered plates and shells embedding functionally graded material layers", *Mech. Adv. Mater. Struct.*, **17**(8), 603-621.
- Cinefra, M. and Soave, M. (2011), "Accurate vibration analysis of multilayered plates made of functionally graded materials", *Mech. Adv. Mater. Struct.*, **18**(1), 3-13.
- Cunedioglu, Y. (2015), "Free vibration analysis of edge cracked symmetric functionally graded sandwich beams", *Struct. Eng. Mech., Int. J.*, **56**(6), 1003-1020.
- Darilmaz, K. (2015), "Vibration analysis of functionally graded material (FGM) grid systems", *Steel Compos. Struct., Int. J.*, **18**(2), 395-408.
- Della Croce, L. and Venini, P. (2004), "Finite elements for functionally graded Reissner–Mindlin plates", *Comput. Methods Appl. Mech. Eng.*, **193**(9-11), 705-725.
- Ebrahimi, F. and Dashti, S. (2015), "Free vibration analysis of a rotating non-uniform functionally graded beam", *Steel Compos. Struct., Int. J.*, **19**(5), 1279-1298.
- Ebrahimi, F. and Habibi, S. (2016), "Deflection and vibration analysis of higher-order shear deformable compositionally graded porous plate", *Steel Compos. Struct., Int. J.*, **20**(1), 205-225.
- Eisenberger, M. and Alexandrov, A. (2003), "Buckling loads of variable thickness thin isotropic plates", *Thin-Wall. Struct.*, **41**(9), 871-889.
- Eltaher, M.A., Alshorbagy, A.E. and Mahmoud, F.F. (2013a), "Determination of neutral axis position and its effect on natural frequencies of functionally graded macro/nanobeams", *Compos. Struct.*, **99**, 193-201.
- Eltaher, M.A., Emam, S.A. and Mahmoud, F.F. (2013b), "Static and stability analysis of nonlocal functionally graded nanobeams", *Compos. Struct.*, **96**, 82-88.
- Eltaher, M.A., Abdelrahman, A.A., Al-Nabawy, A., Khater, M. and Mansour, A. (2014a), "Vibration of

- nonlinear graduation of nano-Timoshenko beam considering the neutral axis position”, *Appl. Math. Computat.*, **235**, 512-529.
- Eltaher, M.A., Khairy, A., Sadoun, A.M. and Omar, F.A. (2014b), “Static and buckling analysis of functionally graded Timoshenko nanobeams”, *Appl. Math. Computat.*, **229**, 283-295.
- Fares, M.E., Elmarghany, M.K. and Atta, D. (2009), “An efficient and simple refined theory for bending and vibration of functionally graded plates”, *Compos. Struct.*, **91**(3), 296-305.
- Ganapathi, M., Prakash, T. and Sundararajan, N. (2006), “Influence of functionally graded material on buckling of skew plates under mechanical loads”, *J. Eng. Mech.*, **132**(8), 902-905.
- Hamidi, A., Houari, M.S.A., Mahmoud, S.R. and Tounsi, A. (2015), “A sinusoidal plate theory with 5-unknowns and stretching effect for thermomechanical bending of functionally graded sandwich plates”, *Steel Compos. Struct., Int. J.*, **18**(1), 235-253.
- Hebali, H., Tounsi, A., Houari, M.S.A., Bessaim, A. and Adda Bedia, E.A. (2014), “A new quasi-3D hyperbolic shear deformation theory for the static and free vibration analysis of functionally graded plates”, *ASCE J. Eng. Mech.*, **140**, 374-383.
- Hosseini-Hashemi, S., Rokni Damavandi Taher, H., Akhavan, H. and Omidi, M. (2010), “Free vibration of functionally graded rectangular plates using first-order shear deformation plate theory”, *Appl. Math. Model.*, **34**(5), 1276-1291.
- Hosseini-Hashemi, S., Fadaee, M. and Atashipour, S.R. (2011a), “A new exact analytical approach for free vibration of Reissner–Mindlin functionally graded rectangular plates”, *Int. J. Mech. Sci.*, **53**(1), 11-22.
- Hosseini-Hashemi, S., Fadaee, M. and Atashipour, S.R. (2011b), “Study on the free vibration of thick functionally graded rectangular plates according to a new exact closed-form procedure”, *Compos. Struct.*, **93**(2), 722-735.
- Houari, M.S.A., Tounsi, A., Bessaim, A. and Mahmoud, S.R. (2016), “A new simple three -unknown sinusoidal shear deformation theory for functionally graded plates”, *Steel Compos. Struct., Int. J.*, **22**(2), 257-276.
- Kang, J.H. and Leissa, A.W. (2005), “Exact solutions for the buckling of rectangular plates having linearly varying in-plane loading on two opposite simply supported edges”, *Int. J. Solids Struct.*, **42**(14), 4220-4238.
- Karama, M., Afaq, K.S. and Mistou, S. (2003), “Mechanical behaviour of laminated composite beam by the new multi-layered laminated composite structures model with transverse shear stress continuity”, *Int. J. Solids Struct.*, **40**(6), 1525-1546.
- Kar, V.R. and Panda, S.K. (2015), “Nonlinear flexural vibration of shear deformable functionally graded spherical shell panel”, *Steel Compos. Struct., Int. J.*, **18**(3), 693-709.
- Kirkland, B. and Uy, B. (2015), “Behaviour and design of composite beams subjected to flexure and axial load”, *Steel Compos. Struct., Int. J.*, **19**(3), 615-633.
- Kitipornchai, S., Yang, J. and Liew, K.M. (2006), “Random vibration of the functionally graded laminates in thermal environments”, *Comput. Methods Appl. Mech. Eng.*, **195**(9-12), 1075-1095.
- Larbi Chaht, F., Kaci, A., Houari, M.S.A., Tounsi, A., Anwar Bég, O. and Mahmoud, S.R. (2015), “Bending and buckling analyses of functionally graded material (FGM) size-dependent nanoscale beams including the thickness stretching effect”, *Steel Compos. Struct., Int. J.*, **18**(2), 425-442.
- Lee, Y.Y., Zhao, X. and Reddy, J.N. (2010), “Postbuckling analysis of functionally graded plates subject to compressive and thermal loads”, *Comput. Methods Appl. Mech. Eng.*, **199**(25-28), 1645-1653.
- Leissa, A.W. (1973), “The free vibration of rectangular plates”, *J. Sound Vib.*, **31**(3), 257-293.
- Leissa, A.W. and Kang, J.H. (2002), “Exact solutions for vibration and buckling of an SS-C-SS-C rectangular plate loaded by linearly varying in-plane stresses”, *Int. J. Mech. Sci.*, **44**(9), 1925-1945.
- Liang, X., Wang, Z., Wang, L. and Liu, G. (2014), “Semi-analytical solution for three-dimensional transient response of functionally graded annular plate on a two parameter viscoelastic foundation”, *J. Sound Vib.*, **333**(12), 2649-2663.
- Liang, X., Wu, Z., Wang, L., Liu, G., Wang, Z. and Zhang, W. (2015), “Semi-analytical three-dimensional solutions for the transient response of functionally graded material”, *ASCE J. Eng. Mech.*, **141**(9), 1943-7889.

- Liu, Y. and Li, R. (2010), "Accurate bending analysis of rectangular plates with two adjacent edges free and the others clamped or simply supported based on new symplectic approach", *Appl. Math. Model.*, **34**(4), 856-865.
- Lu, C.F., Lim, C.W. and Chen, W.Q. (2009), "Semi-analytical analysis for multi-directional functionally graded plates: 3-d elasticity solutions", *Int. J. Numer. Meth. Eng.*, **79**(1), 25-44.
- Mahi, A., Adda Bedia, E.A. and Tounsi, A. (2015), "A new hyperbolic shear deformation theory for bending and free vibration analysis of isotropic, functionally graded, sandwich and laminated composite plates", *Appl. Math. Model.*, **39**(9), 2489-2508.
- Matsunaga, H. (2008), "Free vibration and stability of functionally graded plates according to a 2-D higher-order deformation theory", *Compos. Struct.*, **82**(4), 499-512.
- Meradjah, M., Kaci, A., Houari, M.S.A., Tounsi, A. and Mahmoud, S.R. (2015), "A new higher order shear and normal deformation theory for functionally graded beams", *Steel Compos. Struct., Int. J.*, **18**(3), 793-809.
- Neves, A.M.A., Ferreira, A.J.M., Carrera, E., Cinefra, M., Roque, C.M.C., Jorge, R.M.N. and Soares, C.M.M. (2013), "Static, free vibration and buckling analysis of isotropic and sandwich functionally graded plates using a quasi-3D higher-order shear deformation theory and a meshless technique", *Compos. Part B-Eng.*, **44**(1), 657-674.
- Pradhan, K.K. and Chakraverty, S. (2015), "Free vibration of functionally graded thin elliptic plates with various edge supports", *Struct. Eng. Mech., Int. J.*, **53**(2), 337-354.
- Pradyumna, S. and Bandyopadhyay, J.N. (2008), "Free vibration analysis of functionally graded curved panels using a higher-order finite element formulation", *J. Sound Vib.*, **318**(1-2), 176-192.
- Reddy, J.N. (2000), "Analysis of functionally graded plates", *Int. J. Numer. Methods Eng.*, **47**(1-3), 663-684.
- Shufrin, I. and Eisenberger, M. (2005), "Stability and vibration of shear deformable plates-first order and higher order analyses", *Int. J. Solids Struct.*, **42**(3-4), 1225-1251.
- Sofiyev, A.H. and Kuruoglu, N. (2015), "Buckling of non-homogeneous orthotropic conical shells subjected to combined load", *Steel Compos. Struct., Int. J.*, **19**(1), 1-19.
- Swaminathan, K. and Naveenkumar, D.T. (2014), "Higher order refined computational models for the stability analysis of FGM plates – Analytical solutions", *Eur. J. Mech. A/Solids*, **47**, 349-361.
- Talha, M. and Singh, B.N. (2010), "Static response and free vibration analysis of FGM plates using higher order shear deformation theory", *Appl. Math. Model.*, **34**(12), 3991-4011.
- Talha, M. and Singh, B.N. (2011), "Thermo-mechanical buckling analysis of finite element modelled functionally graded ceramic-metal plates", *Int. J. Appl. Mech.*, **3**(4), 867-880.
- Tounsi, A., Houari, M.S.A., Benyoucef, S. and Adda Bedia, E.A. (2013), "A refined trigonometric shear deformation theory for thermoelastic bending of functionally graded sandwich plates", *Aerosp. Sci. Technol.*, **24**, 209-220.
- Tounsi, A., Houari, M.S.A. and Bessaim, A. (2016), "A new 3-unknowns non-polynomial plate theory for buckling and vibration of functionally graded sandwich plate", *Struct. Eng. Mech., Int. J.*, **60**(4), 547-565.
- Tung, H.V. (2015), "Thermal and thermomechanical postbuckling of FGM sandwich plates resting on elastic foundations with tangential edge constraints and temperature dependent properties", *Compos. Struct.*, **131**, 1028-1039.
- Wang, X., Gan, L. and Wang, Y. (2006), "A differential quadrature analysis of vibration and buckling of an SS-C-SS-C rectangular plate loaded by linearly varying inplane stresses", *J. Sound Vib.*, **298**(1-2), 420-431.
- Xiang, S., Jin, Y.-x., Bi, Z.-y., Jiang, S.-x. and Yang, M.-s. (2011), "A n-order shear deformation theory for free vibration of functionally graded and composite sandwich plates", *Compos. Struct.*, **93**(11), 2826-2832.
- Xiao, J.R., Batra, R.C., Gilhooley, D.F., Gillespie Jr., J.W. and McCarthy, M.A. (2007), "Analysis of thick plates by using a higher-order shear and normal deformable plate theory and MLPG method with radial basis functions", *Comput. Methods Appl. Mech. Eng.*, **196**(4-6), 979-987.
- Yang, J., Liew, K.M. and Kitipornchai, S. (2005), "Stochastic analysis of compositionally graded plates with system randomness under static loading", *Int. J. Mech. Sci.*, **47**(10), 1519-1541.
- Zenkour, A.M. (2006), "Generalized shear deformation theory for bending analysis of functionally graded

- plates”, *Appl. Math. Model.*, **30**(1), 67-84.
- Zhao, X. and Liew, K.M. (2009), “Geometrically nonlinear analysis of functionally graded plates using the element-free kp-Ritz method”, *Comput. Methods Appl. Mech. Eng.*, **198**(33-36), 2796-2811.
- Zhao, X., Lee, Y.Y. and Liew, K.M. (2009), “Free vibration analysis of functionally graded plates using the element-free kp-Ritz method”, *J. Sound Vib.*, **319**(3-5), 918-939.
- Zidi, M., Tounsi, A., Houari, M.S.A., Adda Bedia, E.A. and Anwar Bég, O. (2014), “Bending analysis of FGM plates under hygro-thermo-mechanical loading using a four variable refined plate theory”, *Aerosp. Sci. Technol.*, **34**, 24-34.

CC